

RESEARCH ARTICLE

 OPEN ACCESS

Received: 07-09-2023

Accepted: 08-10-2023

Published: 06-12-2023

Citation: Anbalagan S, Ravishankar M, Sivakumar S, Sivakumar M, Krishnan E (2023) Corrosion Inhibition of Mild Steel by Newly Synthesized 1-[(4-nitrophenyl)methyl]-4-(pyridin-2-yl)piperazine in HCl Acid Medium. Indian Journal of Science and Technology 16(45): 4211-4224. <https://doi.org/10.17485/IJST/v16i45.2276>

* **Corresponding author.**

ravishankar1in@yahoo.co.in

Funding: None

Competing Interests: None

Copyright: © 2023 Anbalagan et al. This is an open access article distributed under the terms of the [Creative Commons Attribution License](https://creativecommons.org/licenses/by/4.0/), which permits unrestricted use, distribution, and reproduction in any medium, provided the original author and source are credited.

Published By Indian Society for Education and Environment ([iSee](https://www.isee.org/))

ISSN

Print: 0974-6846

Electronic: 0974-5645

Corrosion Inhibition of Mild Steel by Newly Synthesized 1-[(4-nitrophenyl)methyl]-4-(pyridin-2-yl)piperazine in HCl Acid Medium

S Anbalagan^{1,2}, M Ravishankar^{1*}, S Sivakumar³, M Sivakumar³, E Krishnan⁴

1 Department of Chemistry, Rajah Serfoji Government College, Affiliated to Bharathidhasan University, Thanjavur, 613005, Tamil Nadu, India

2 Department of Chemistry, Laxminarayana College of Arts & Science (women), Dharmapuri, Tamil Nadu, India

3 Department of Chemistry, E. R. K Arts and Science College, Dharmapuri, Tamil Nadu, India

4 Department of Chemistry, P.S.A Arts and Science College, Dharmapuri, Tamil Nadu, India

Abstract

Objectives: To use the newly synthesized efficient organic corrosion inhibitor 1-[(4-nitrophenyl)methyl]-4-(pyridin-2-yl)piperazine (NMPP) to carry out on mild steel corrosion inhibition study. **Methods:** The 1-[(4-nitrophenyl)methyl]-4-(pyridin-2-yl)piperazine (NMPP) organic inhibitor was synthesized by condensation polymerization. The organic inhibitor NMPP, was characterized by Fourier transform infrared (FTIR), and high resolution scanning electron microscope (HR-SEM). The inhibition action of the polymer composite was investigated by conventional weight loss method, and electrochemical impedance spectroscopy (EIS). **Findings:** The maximum corrosion inhibition efficiency of 88.34 % was obtained at concentration level of 6 % at 303K. The results revealed NMPP as a mixed type corrosion inhibitor, the thermodynamic and kinetic parameters also revealed adsorption of catalyst on to mild surface as exothermic and the adsorption was confirmed by conventional weight loss method. **Novelty:** FT-IR analysis reveals that predominant peaks are the interaction between inhibitor and mild steel surfaces. The morphology of mild steel coupons was investigated by HR-SEM. The HR-SEM results showed novel inhibitor to have inhibited corrosion on mild steel in 1 M HCL on CO₂ environment.

Keywords: Novel inhibitor; Mild steel; HRSEM; NMPP and Corrosion Inhibition

1 Introduction

Corrosion inhibitors are substances used to prevent or reduce metal surface corrosion in corrosive environments. There are two types of corrosion inhibitors: natural and synthetic⁽¹⁾. Natural inhibitors, derived from plants and minerals, are eco-friendly,

biodegradable, and low in toxicity. Examples include vegetable oils, tannins, and salicylic acid. However, they may have limited effectiveness and may be unsuitable for severe corrosion environments. Furthermore, their costs can be higher compared to synthetic inhibitors⁽²⁾. Despite these limitations, natural inhibitors are gaining popularity as sustainable and eco-friendly alternatives to synthetic inhibitors that can be used in various applications, such as in the oil and gas industry and for preserving historical artifacts⁽³⁾. Natural inhibitors are renewable, biodegradable, and safe for human exposure, making them appropriate for industries such as food and pharmaceuticals⁽⁴⁾.

In contrast, synthetic inhibitors are chemically manufactured to provide high efficacy in a range of corrosive environments. Amines salts, phosphates, and nitrites are examples of synthetic inhibitors⁽⁵⁾. Synthetic inhibitors are more effective, have a wider range of applications, are reliable, and have a longer shelf life than natural inhibitors⁽⁶⁾. Synthetic inhibitors form a protective film on metal surfaces and react with corrosive substances to prevent corrosion. They are particularly effective in harsh and corrosive environments with high levels of impurities, salt, and other contaminants⁽⁷⁾.

Synthetic inhibitors are ideal for applications such as offshore platforms, pipelines, and nuclear power plants where maintenance is challenging or costly. Nevertheless, synthetic inhibitors are more expensive than natural inhibitors and require proper selection and dosing to prevent environmental damage and interference with other chemical processes in the system⁽⁸⁾. In summary, synthetic inhibitors are widely used in various industrial applications due to their effectiveness, but their potential environmental impact should be considered, and their selection and dosing should be carefully managed⁽⁹⁾.

Organic inhibitors are preferably used over inorganic inhibitors due to their cheap availability and also, they are less toxic compare to inorganic inhibitors⁽¹⁰⁾. Organic inhibitors with heterocyclic organic structures containing pi conjugated structure and heteroatoms, like N, S, O and P, capable of adsorbing on the metal surfaces via physisorption or chemisorption adsorption, are often being most effective⁽¹¹⁾. Commonly adopted corrosion inhibitors are organic compounds including quinoline, piperazine and their derived salts^(12,13).

The literature reports that the corrosion rate in chlorides containing fluids increases exponentially in the presence of CO₂. The use of corrosion inhibitors is one of the most cost-effective and practical methods for controlling CO₂ corrosion in the oil and gas industry. The typical commercial inhibitors so far used in the oil/gas field to inhibit CO₂ corrosion occurring in internal carbon steel pipelines are nitrogen-based compounds⁽¹⁴⁾. The literature reports that these inhibitors exhibit excellent anti-corrosion properties. However, some of these inhibitors were recognized from the Environment European Commission (EEC) as toxic and potentially dangerous to both the environment and human health. Due to these serious threats, the EEC, with the directive 76/464/EEC, has therefore limited the use of such inhibitors. These concerns have led many researchers to focus their studies toward the development of more environmentally friendly corrosion inhibitors for CO₂ corrosion of the steel.

A novel heterocyclic compounds tert-butyl 4-[(4-methyl phenyl) carbonyl] piperazine-1-carboxylate [TBMPCPC]. Electrochemical, quantum chemical, and surface characterization studies at elevated temperatures (303–333 K) for carbon steel in 1M HCl solution studied this molecule's corrosion inhibition property. It is observed from the results of electrochemical studies that the⁽¹⁵⁾ TBMPCPC may be able to effectively protect the steel plate surface with an inhibition efficiency of 91.5 % at 25 ppm in corrosive media. Majid R. et al., introduced 1,4-bis(2-(2-hydroxyethyliminomethyl)phenyl)piperazine and 1,4-bis(2-(2 hydroxyethylaminomethyl)phenyl)piperazine as effective corrosion inhibitor for carbon steel in 1.0 M HCl solutions,⁽¹⁶⁾

In view of the aforementioned, the present work was designed towards the investigation of piperazine derivatives with potentially high inhibition efficiencies at relatively low concentrations. The protection performances of carboxamide derivatives namely, 1-[(4-nitrophenyl)methyl]-4-(pyridin-2-yl)piperazine (NMPP) for mild steel in HCl medium are hereby reported. Corrosion inhibition efficiency of mild steel was tested against the mild steel in presence of 1N HCl and was analyzed with the aids of weight loss method.

2 Methodology

2.1 Materials

1-(pyridin-2-yl)piperazine, 98.0%; 4-nitrobenzaldehyde, 98.5% ; 1,2-dichloroethane were purchased from Merck chemicals Ltd. Sodiumtriacetoxo borohydride, 99.0%; and other reagents and solvents were purchased from HiMedia Laboratories Pvt. Ltd. (Mumbai, India). All the chemicals were used without further purification. All aqueous solutions were prepared with nanopure water. All apparatus and glassware's are washed with acetone, rinsed with deionized water (DIW) and dried with air hot oven at 100 °C, then it was used throughout the studies.

2.2 Methods

2.2.1 Synthesis of 1-[(4-nitrophenyl)methyl]-4-(pyridin-2-yl)piperazine (NMPP)

The 1-[(4-nitrophenyl)methyl]-4-(pyridin-2-yl)piperazine (NMPP) corrosion inhibitor have been synthesized with help of our previous report⁽¹⁷⁾.

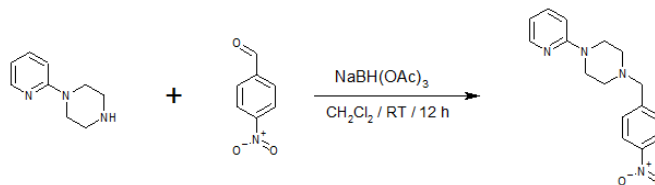


Fig 1.

A dry 250 mL round bottom flask with magnetic stirring bar was charged consecutively with 1-(pyridin-2-yl)piperazine (5 g, 0.036 mol), 4-nitrobenzaldehyde (5.1 g, 0.033 mol) and 1,2-dichloroethane (100 mL) in nitrogen atmosphere then treated with sodium triacetoxy borohydride (9.7 g, 0.046 mol). The resulting reaction mixture was stirred at RT under a Nitrogen atmosphere for 12 hr. The progress of the reaction was monitored by TLC. The reaction mass was quenched by adding aqueous saturated NaHCO₃ (50 mL), and extracted with ethyl acetate (2x150 mL). The combined organic layer was washed with water (1x200 mL), saturated NaCl (1x300 mL), dried over Na₂SO₄ and the solvents were removed under reduced pressure. We get pale yellow crystalline solid, 7.38 g. In this product is used as a catalyst for corrosion inhibition for mild steel at elevated temperature in CO₂ medium.

2.2.2 Steel sample preparation

The mild steel specimens (50.00 mm 25.00 mm 1.5.00 mm: length, width, height) were purchased from JSWSTEEL Co., Ltd., (Tamilnadu, India) with chemical composition (wt%) of 0.098 P; 0.36 Si; 0.53 Mn; 0.20 C; 0.011 S and the remaining Fe. The mild steel specimen was ground with different emery papers (grade 200, 400, 600 and 800) in order to abrade the surface of mild steel from impurities and for more smoothing for investigation, rinsed with double distilled water, degreased with acetone before use, dried and kept in a desiccator at room temperature.

2.2.3 Inhibitors and solutions

The corrosive solutions of 1 N HCl were prepared by dilution of analytical grade 37% HCl with double distilled water. The acid solutions for weight loss and electrochemical measurements were used without and with various concentrations of NMPP at room temperature.

2.2.4 Weight Loss Experiment

The weight loss experiments were performed for duration of 6 h, as per ASTM designation G1-90. The clear and dry specimen was measured for the total surface area with utmost accuracy. The specimen was weighed accurately by a digital balance with a sensitivity of ± 0.1 mg balance. To hold the specimen, a hole with a diameter of 1.5 mm was made near the edge of the specimen. After taking the initial weight and dimensions, the freshly prepared mild steel specimens were suspended into 100 ml beakers containing 90 ml of test solution maintained at room temperature with the aid of glass rods and hooks. To avoid crevice corrosion, the specimens were hanged in the test solution with the help of nylon thread. A blank experiment was also carried out for the comparison purpose. The studies were carried out under varying concentrations inhibitors at room temperature. The experimental conditions were controlled in order to ensure reproducible results. After a definite immersion period, the steel specimen was taken out and washed with running water. The corrosion product was removed mechanically by rubbing with brush on the steel surface. The steel specimen was then dried and the loss in weight was recorded by weighing.

The corrosion rates were determined using the Equation (2.1).

$$CR = \frac{87.6 W}{atd} \times 100 \quad (2.1)$$

where W is the weight loss (mg), 'a' represents the exposed area (cm²), t refers to the exposed time (h), and 'd' is the stripes density (g. cm⁻³).

The percentage inhibition efficiency (% IE) was calculated by using the following equation:

$$\%IE = \frac{CR_o - CR_i}{CR_o} \times 100 \quad (2.2)$$

Where, CR_o is the corrosion rate of mild steel in absence of inhibitor and CR_i is the corrosion rate of mild steel in presence of inhibitor.

2.2.5 Electrochemical measurements

For all corrosion experiments, a traditional 3 electrode device was plugged into the CHI608D electrochemical workstation for the electrochemical experiments. The three electrode device consisted of a working electrode carbon steel strip, a counter electrode platinum electrode and a saturated calomel electrode as a reference electrode. For electrochemical measurements, a polished working electrode with an exposed area of 1 cm^2 (the remainder of the portion was covered by epoxy resin) was used.

The mild steel (working electrode) was dipped in the sample solution for about 30 min for the open circuit potential (OCP) to enter the steady state before performing the electrochemical experiment. The potentiodynamic polarisation curves were obtained within the potential range of +0.2 to -0.2 mV (vs. SCE) with a scan rate of 1.0 mV s^{-1} . Electrochemical parameters such as corrosion potential (E_{corr}), corrosion current densities (i_{corr}), and Tafel slopes (β_c, β_a) can be derived by extrapolation of the linear Tafel segments of the polarization curves.

Electrochemical impedance study also carried out the same electrochemical workstation with frequency range from 10kHz to 0.01 Hz were fixed with an appropriate equivalent circuit using analyst software and 10 mV amplitude using with open circuit potential all impedance data. The inhibitor efficiency $\eta\%$ was calculated from charge transfer resistance value obtained from impedance measurement using following relation.

$$\eta\% = \frac{R_{ct}(\text{inh}) - R_{ct}}{R_{ct}(\text{inh})} \times 100$$

R_{ct} – charge transfer resistance in presence and absence of inhibitor respectively.

The values of double layer were calculated from the following equation $C_{dl} = (mF \times 10^{-5}) 1/n$

2.2.6 Mild Steel Surface Analyses

Corroded mild steel surface obtained after immersion in the 1 N HCl solution with and without the optimal concentration of inhibitors was analyzed using scanning electron microscope. AFM was done using a Bruker MULTIMODE instrument. AFM was conducted using a tapping mode and a 2.5 Hz scan rate.

2.2.7 Characterization methods

The high resolution scanning electron microscopy (HR-SEM) was carried out on a FEI Quanta FEG 200 instrument facility at 25°C . The sample was prepared by placing a small quantity of the prepared material on a carbon coated copper grid and allowing the solvent to evaporate. FT-IR spectra were recorded with thermo scientific spectrometer, model no. iS5 equipped with attenuated total reflectance (ATR) facility which is implemented with Zn-Se crystal detector. Each spectrum was recorded with an acquisition time of 18 s. The FT-IR measurement was scanned at a range from 4000 to 400 cm^{-1} .

3 Results and discussion

3.1 FT-IR analysis

The FT-IR spectra of the bare NMPP and NMPP inhibited mild steel were shown in Figure 2. The FT-IR spectrum of the Figure 2a indicates the absorption band of pure NMPP. These bands pronounced at 3172.4 cm^{-1} and 1546.2 cm^{-1} subsequent to stretching and bending vibration of the absorbed water molecules respectively shown in Figure 2a. The main absorption peaks at 534.2 , 709.3 and 978.0 cm^{-1} was assigned to the C-C, C-N, N-O and C-N-C bending vibrations respectively⁽¹⁸⁾. Figure 2b shows the absorption peak at 3092.6 - 3202.6 cm^{-1} be assigned to the stretching vibration of surface $^{-}\text{O}_2\text{N}$ group attributed to the blue shifted region due to the interaction between the C-N and Nitro groups. The most important absorption peaks at 2865.4 and 1060.9 cm^{-1} was assigned to the stretching vibration of N-H, CH_2 respectively⁽¹⁹⁾. Fe-O-N and Fe-NH bonds of the Mild Steel sample emerged at 1343.6 and 1540.5 cm^{-1} respectively.

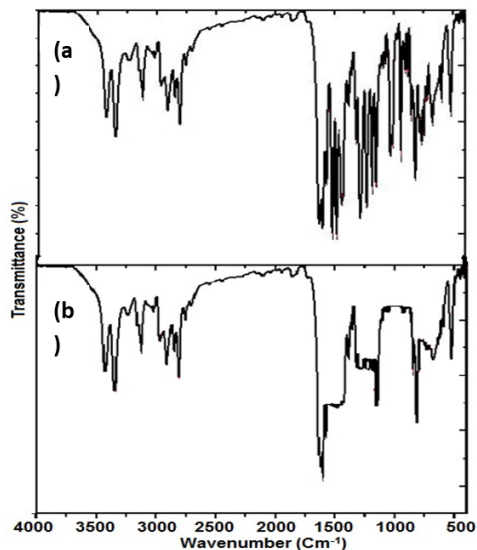


Fig 2. FT-IR spectra of (a) bare NMPP, (b) MS interacted NMPP surfaces

3.2 Corrosion inhibition efficiency analysis at 303K

The corrosion rate of mild steel in 1N Hydrochloric acid at various temperatures has been studied by weight loss method⁽²⁰⁾. The rate of corrosion obtained from weight loss studies are given in Table 1. From the table, the corrosion rate of mild steel in 1N Hydrochloric acid is found to be increasing with increasing in temperature from 303 K-333 K, indicates that the increasing in temperature enhanced the interaction between metal surface and acidic medium. It has been evident from the straight-line behavior obtained by plotting a graph with corrosion rate Vs temperatures ranges between 303 K-333 K as shown in Figure 3.

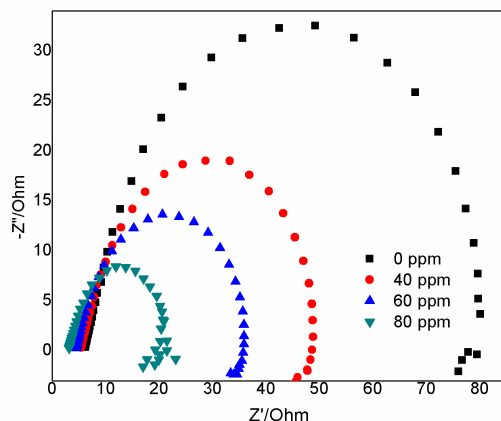


Fig 3. Impedance curves of mild steel electrode soaked in 1N HCl in the absence and presence of the NMPP inhibitor at 303K

The corrosion behavior of mild steel in 1N Hydrochloric acid after the addition of 20 ppm to 100 ppm of NMPP at room temp in 6 hours has been studied. The corrosion rates, inhibitor efficiency and surface coverage are calculated as shown in Table 1. It can be seen that corrosion rate of mild steel decreases with increasing percentage of NMPP concentration up to 6 % when compared with 0% of NMPP concentration. The rate of corrosion of mild steel in 1N Hydrochloric acid decreases with increasing % of NMPP. It indicates that the inhibition of NMPP is found to be effective up to 6%, since it increases that rate of corrosion as given in Table 1.

It is evident from the graph obtained by plotting percentage of NMPP against the rate of corrosion that the addition of NMPP concentration 20 ppm to 100 ppm is found to be effective at room temp in three hours as shown in Figure 4. From the Table 1, it is also observed that the inhibitor efficiency and surface coverage are found to increase with respect to the concentration of inhibitor increase up to 80 ppm of the inhibitor from the mild steel surfaces. It is also found that the maximum inhibitor efficiency is 88.34% at room temperature. It is also evident from the graph obtained by plotting percentage of inhibitor efficiency and surface coverage against percentage of inhibitor as shown in Figure 4.

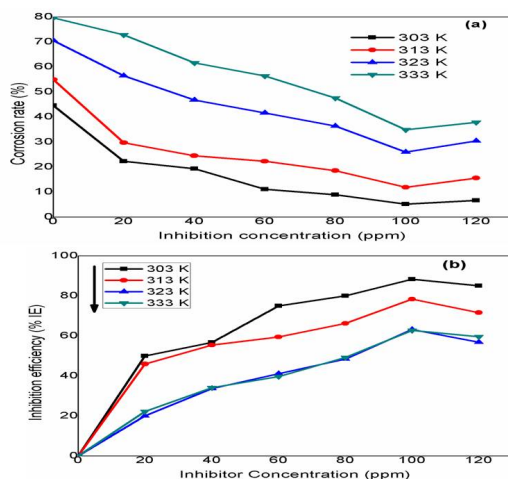


Fig 4. Comparisons of corrosion inhibition rates at up to 303K-333K of (a) concentration of inhibitor vs corrosion inhibition rates, (b) concentration of inhibitor vs corrosion inhibition efficiency

3.2.1 Corrosion inhibition efficiency analysis at 313K

The corrosion behavior of mild steel in 1N Hydrochloric acid after the addition of 20 ppm to 100 ppm of NMPP at 313 K in 6 hours has been studied. The corrosion rates, inhibitor efficiency and surface coverage are calculated shown in Table 1. It can be seen that corrosion rate of mild steel decrease with increasing percentage of NMPP in upto 80 ppm when compared with 0 ppm of NMPP. The rate of corrosion of mild steel in 1N Hydrochloric acid decreases with increasing % of NMPP concentration. It indicates that the inhibition of NMPP is found to be effective in 80 ppm of NMPP concentration. Since it increases that the rate of corrosion as given in Table 1. It is evident from the graph obtained by plotting percentage of NMPP concentration against the rate of corrosion that the addition of NMPP in 6% is found to be effective at 313 K in five hours as shown in Figure 4.

From the Table 1 it is also observed that the inhibitor efficiency is found to increase with respect to the concentration of inhibitor increase in 80 ppm. It is also found that the maximum inhibitor efficiency 78.37% at 323 K. It is also evident from the graph obtained by plotting percentage of inhibitor efficiency against percentage of inhibitor as shown in Figure 4. It was assumed that the inhibitor efficiency is equal to surface coverage (Θ) from Table 1. It is observed that the surface coverage (Θ) is found to be increased in 80 ppm

3.2.2 Corrosion inhibition efficiency analysis at 323K

The corrosion behavior of mild steel in 1N Hydrochloric acid after the addition of 20 ppm to 100 ppm of NMPP concentrations at 323 K in 6 hours has been studied. The corrosion rates, inhibitor efficiency and surface coverage are calculated shown in Table 1. It can be seen that corrosion rate of mild steel decrease with increasing percentage of NMPP concentration up to 80 ppm when compared with 0 ppm of NMPP concentration.

The rate of corrosion of mild steel in 1N Hydrochloric acid decreases with increasing % of NMPP concentrations. It indicates that the inhibition of NMPP is found to be effective on 80 ppm of NMPP concentration, since it increases that rate of corrosion as given in Table 1. It is evident from the graph obtained by plotting percentage of NMPP concentrations against the rate of corrosion that the addition of NMPP concentrations up to 6 % is found to be effective at 323 K in three hours as shown in Figure 4. From the Table 1 it is also observed that the inhibitor efficiency is found to increase with respect to the concentration of inhibitor increase up to 80 ppm. It is also found that the maximum inhibitor efficiency 63.15% at 323 K. It is also evident from the graph obtained by plotting percentage of inhibitor efficiency against percentage of inhibitor as shown in Figure 4.

3.2.3 Corrosion inhibition efficiency analysis at 333K

The corrosion behavior of mild steel in 1N Hydrochloric acid after the addition of 20 ppm to 100 ppm of NMPP at 333 K in 6 hours has been studied. The corrosion rates, inhibitor efficiency and surface coverage are calculated shown in Table 1. It can be seen that corrosion rate of mild steel decrease with increasing percentage of NMPP concentration in 80 ppm when compared with 0 ppm of NMPP. The rate of corrosion of mild steel in 1N Hydrochloric acid decreases with increasing % of NMPP concentrations. It indicates that the inhibition of NMPP is found to be effective in 80 ppm of NMPP concentration. Since it increases the rate of corrosion as given in Table 1. It is evident from the graph obtained by plotting percentage of NMPP concentrations against the rate of corrosion that the addition of NMPP in 6 % is found to be effective and above is found to be less effective at 333 K in five hours as shown in Figure 4.

From the Table 1 it is also observed that the inhibitor efficiency is found to increase with respect to the concentration of inhibitor increase in 80 ppm. It is also found that the maximum inhibitor efficiency 62.69% at 333 K. It is also evident from the graph obtained by plotting percentage of inhibitor efficiency against percentage of inhibitor as shown in Figure 4. It was assumed that the inhibitor efficiency is equal to surface coverage (Θ) from Table 1. It is observed that the surface coverage (Θ) is found to be increased in 80 ppm.

3.2.4 Comparison of corrosion inhibition efficiency analysis at 303K - 333K

The effect of temperature on inhibition of mild steel corrosion in 1N Hydrochloric acid with 20 ppm to 100 ppm of NMPP concentrations between the temperature ranges from room temperature to 333 K has been studied and the results were calculated as in Table 1.

Table 1. Comparison of corrosion inhibition efficiency analysis at 303K - 333K

S.No	Concentration of NMPP (%)	Initial weight (g)	Final weight (g)	Weight Loss (mg)	Corrosion Rate (mmpy)	Inhibitor Efficiency (%)	Surface Coverage (Θ)
Room Temperature (303K)							
1	0	12.988	12.928	60	44.58	0	0
2	20	13.23	13.2	30	22.29	50	0.5
3	40	13.521	13.495	26	19.32	56.67	0.57
4	60	12.391	12.976	15	11.15	75	0.75
5	80	14.117	14.105	12	8.92	80	0.8
6	100	14.559	14.552	7	5.2	88.34	0.88
7	120	13.981	13.972	9	6.69	85	0.85
(313K)							
1	0	13.029	12.955	74	54.98	0	0
2	20	13.38	13.34	40	29.72	45.94	0.459
3	40	13.751	13.718	33	24.52	55.4	0.554
4	60	13.048	13.018	30	22.29	59.45	0.595
5	80	13.766	13.741	25	18.58	66.21	0.662
6	100	12.751	12.735	16	11.89	78.37	0.784
7	120	13.004	12.983	21	15.6	71.62	0.716
(323K)							
1	0	13.522	13.427	95	70.59	0	0
2	20	13.655	13.579	76	56.47	20	0.2
3	40	13.192	13.129	63	46.8	33.68	0.337
4	60	13.667	13.611	56	41.61	41.05	0.411
5	80	13.292	13.243	49	36.41	48.42	0.484
6	100	12.963	12.928	35	26.01	63.15	0.632
7	120	12.082	12.941	41	30.46	56.84	0.568
(333K)							
1	0	13.14	13.266	126	79.62	0	0
2	20	13.327	13.425	98	72.81	22.23	0.222
3	40	13.323	13.406	83	61.67	34.12	0.341
4	60	13.288	13.364	76	56.41	39.68	0.397
5	80	13.259	13.323	64	47.55	49.2	0.492
6	100	13.984	14.031	47	34.92	62.69	0.627
7	120	13.109	13.16	51	37.89	59.52	0.595

From the Table 1, it is seen that the rate of corrosion of mild steel in 1N Hydrochloric acid with 20 ppm to 100 ppm of NMPP concentration increases with respect to temperature. It is also observed that the rate of corrosion is found to be decreased up to 80 ppm of the NMPP. It indicates that the NMPP is found to be more effective in inhibition of mild steel corrosion in 1N Hydrochloric acid up to 80 ppm at 303 K - 333K. It is also evident from the graph obtained by plotting percentage of NMPP against the rate of corrosion as shown in Figure 4. From the Table 1, it is also observed the NMPP is an effective inhibitor in inhibition of mild steel corrosion in 1N Hydrochloric acid up to 80 ppm of concentration at room temperature. It indicates that the NMPP is stable only at room temperature since the efficiency observed is 88.34 % at room temperature and the surface coverage is equal to the inhibitor efficiency.

Some corrosion inhibition study was compared with recent reports.⁽²¹⁾ Lavanya DK et al., was tested the corrosion inhibition efficiency of (1E)-benzylidene hydrazine on mild steel in 0.5 M HCl at temperatures 303, 313, 323, and 333 K. The inhibition efficiency was found to increase with an increase in the inhibitor concentration. The maximum inhibition efficiency of 92% was observed for 500 ppm of the inhibitor at 323 K. The corrosion resistance of 2-amino-4-phenyl-2H-pyrano[3,2-h]quinolin-3-carbonitrile (QP-H) to mild steel in 1 M HCl solution at different temperatures (298–328 K) has been studied by⁽²²⁾ M. Oubaaqa et al. The electrochemical results show that as the concentration of the corrosion inhibitor increases, the inhibition efficiency also increases. A triazole heterocyclic compound namely 3-(4-ethyl-5-mercapto-1, 2, 4-triazol-3-yl)-1-phenylpropanone (EMTP) was examined for its corrosion protection of mild steel (MS) against 1 M hydrochloric acid medium using gravimetric techniques.⁽²³⁾ Alkadir Aziz, I. A et al. found excellent corrosion protection performance of EMTP at low and high concentrations towards MS in HCl solution. EMTP has potential corrosion inhibitor for mild steel with the highest protection efficacy of 97% at 303 K.⁽²⁴⁾ Yuhao Chen et al., synthesized corrosion inhibitor like 3-morpholino-1- phenyl-3-(pyridin-4-yl) propan-1-one (MPPO) for the mild steel corrosion inhibition purpose. The inhibition efficiency was increased with the increase in inhibitor concentrations, with the corrosion inhibition efficiency reaching 91.4%, at a concentration of 300 ppm at 305 K.

Table 2. The comparison of corrosion inhibition performance of NMPP inhibitor with reported heterocyclics derivatives

Heterocyclics derivatives	Corrosive medium	Concentration	Temperature	Inhibition efficiency (IE%)	References
(1E)-benzylidene hydrazine)	0.5 M HCl	500 ppm	323 K	92 %	Lavanya et.al., ⁽²¹⁾ DK
2-amino-4-phenyl-2H-pyrano[3,2-h]quinolin-3-carbonitrile (QP-H)	1 M HCl	-	298-328	92%	M. Oubaaqa et.al., ⁽²²⁾
3-(4-ethyl-5-mercapto-1, 2, 4-triazol-3-yl)-1-phenylpropanone (EMTP)	1.0 M HCl	0.5 mmol L-1	303 K	97%	Alkadir Aziz, I. A et.al. ⁽²³⁾
3-morpholino-1- phenyl-3-(pyridin-4-yl) propan-1-one (MPPO)	1 M HCl	300 ppm	305K	91.4%,	Yuhao Chen et.al., ⁽²⁴⁾
N-(4-((4-(pyridin-2-yl)piperazin-1-yl)methyl)phenyl)isonicotinamide (NPPMPIA)	1 N HCl	6%	303K	90.39%	Present work

Compared to above reviews NMPP possess the maximum inhibition efficiency in 1N hydrochloric acid as found to be 88.34% at 303K for 6% of concentration.

3.3 Electrochemical Studies

3.3.1 Electrochemical Impedance Spectroscopy

The inhibition efficiency of the inhibitor was investigated by Electrochemical Impedance Spectroscopy (EIS), which is also a good appropriate technique. This technique clearly explains the adsorptive nature of the NMPP inhibitor over the mild steel surface in 1N HCl medium (Figure 4). For diverse corrosion system features of EIS Spectra had been validated based totally on their charge transfer control, diffusion control of inhibitor. From Nyquist plot (EIS data), the mechanism of corrosion may be diagnosed. An electrochemical interface which in term referred as electrical features may be interpreted the usage of EIS information. In homogeneity of the surface and roughness of the electrodes recurrently refers to frequency dispersion. The

depressed semicircle with the center under beneath the actual axis of Nyquist plot presentation the characteristic for solid electrodes⁽²⁵⁾. Nyquist plots for interface of mild steel electrode and electrolyte in non-existence and the existence of inhibitor at various concentrations shown in Figure 3. Impedance parameters were exemplified in Table 3. The presence of the N-H group and phenyl group in the inhibitor compound shows a better efficacy on prevention of mild steel material.

Table 3. Impedance parameters of mild steel electrode soaked in 1N HCl without and with inhibitor at room temperature

S.No	Inhibitor concentration (ppm)	Rct(ohm cm ²)	Cdl(mF X10 ⁻⁵)	Inhibition (%)	Efficiency
1	Blank	16.22	89.23	-	
2	20	32.48	73.23	30.2	
3	40	55.43	35.40	45.66	
4	80	88.90	22.40	74.34	

The fitted solid lines in Figure 3 using the open electric circuit of Figure 5 are in accordance with EIS test data, indicating that the equivalent circuit can be used to fit the experimental data. Rs is the solution resistance, Rct is the charge transfer resistance and Cdl represents the double layer charge, of the adsorption characteristics of inhibitor on the electrode surface.

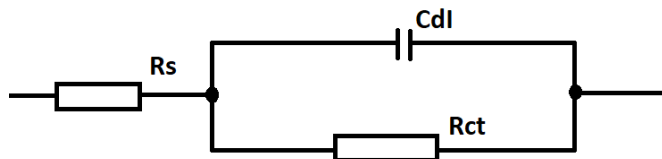


Fig 5. Open circuit model used to fit impedance spectra

3.3.2 Potentiodynamic tafel polarisation measurements

The electrochemical Tafel polarisation curves for mild steel without and with the addition of different concentrations of NMPP in 1N HCl at 303 K are shown in Figure 6.

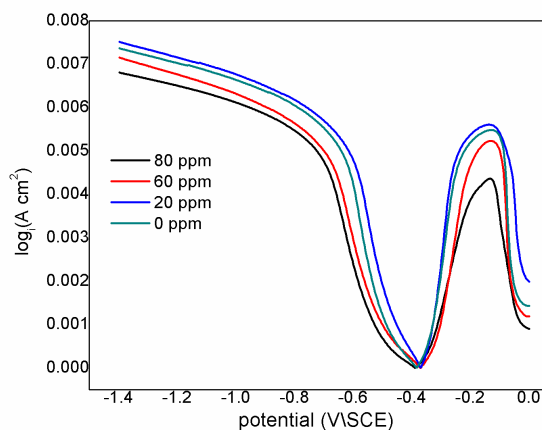


Fig 6. Electrochemical Tafel polarisation curves for mild steel without and with the addition of different concentrations of NMPP in 1M HCl

The graph of current against potential was plotted at the given potential range at the scan rate of 0.01 mV/s. Table 4 consists of corrosion parameters viz., corrosion potential (E_{corr}), corrosion current density (i_{corr}), Corrosion rate (v) and inhibition efficiency (η_p). The inhibition efficiency of NPPMPQC for mild steel in 1N HCl is computed by the following expression⁽¹⁵⁾,

The inhibition efficiency (IE, %) from potentiodynamic polarization was calculated using the following equation:

$$\%IE = \frac{I_0 - I'}{I_0} \times 100 \quad (3.3)$$

where I_0 and I' are the corrosion current density without and with the inhibitor, respectively. The results show that with increasing NMPP concentrations, the corrosion rate is gradually decreasing. This is due to the accumulation of NMPP by adsorption from the bulk solution onto the metal surface.

Table 4. Corrosion parameters like corrosion potential (E_{corr}), corrosion current density (i_{corr}), Corrosion rate (v) and inhibition efficiency (η_p)

S.No	Inhibitor (ppm)	Concentration	E_{corr} (V)	i_{corr} (A) (A)	Corrosion rate (mm/year)	Inhibition (%)	Efficiency
1	0		-0.3593	0.0002	2.5625	-	
2	20		-0.36917	0.00018919	2.1984	31.23	
3	40		-0.3836	0.0002	1.6833	40.23	
4	80		-0.37054	0.00009	1.0679	75.43	

The adsorbed molecules on metal surfaces block the corrosion sites, which reduce the rate of corrosion. It is also stated that the corrosion rate (v) decreases with the increasing concentration of inhibitor in 1N HCl. From the above data, it is concluded that the corrosion inhibition efficiency also increases for mild steel in 1N HCl solution as the concentration of the inhibitor increases. Therefore, NMPP exhibits high inhibition efficiency, but due to the destruction of adsorbed layers over the mild steel surfaces, inhibition efficiency decreases with the increasing inhibitor concentration.

3.3.3 Corrosion Mechanism

Details on the interaction between inhibitor molecules and the mild steel surface are needed to characterize the inhibition mechanism. In an acidic solution, mild steel is positively charged, and the inhibitor molecules are either neutral or protonated. As stated earlier, it is difficult to understand how inhibitor molecules adsorb; they may do so in several ways. As a result of a synergistic interaction with pre-adsorbed NO_2^- , the protonated sites of inhibitor molecules leap to adsorb on the metal surface.

Inhibitor molecules that are positively charged begin competing with H^+ for electrons on the MS surface and, after liberating H_2 ,⁽¹⁶⁾ transition back to the neutral state where they are ready to accept empty d orbitals of iron atoms. The iron's d orbital's excess negative charges can be transferred to the empty (antibonding) of inhibitor molecules, accumulating extra negative charges on the mild steel surface.

3.3.4 Adsorption Isotherm

The communal effects between inhibitors and the metallic surface are able to be examined over the adsorption isotherm since inhibitors normally adsorb upon the metal/solution surface.

Among various adsorption isotherms (Langmuir, Frumkin, Temkin), Langmuir adsorption isotherm displays the finest explanation for the adsorption behavior of the investigated inhibitors since the correlation coefficient (R^2) were close to 1. Langmuir isotherm and corresponding adsorption thermodynamics parameters can be conveyed by the following Equation (3.4).

$$\frac{C}{\theta} = \frac{1}{K_{abs}} + C \quad (3.4)$$

$$K_{abs} = \frac{1}{55.5} \exp \left(\frac{-\Delta G_{ads}}{RT} \right)$$

where C shows the concentration of inhibitors; θ stands for surface coverage, whose value has been calculated by weight loss test; K_{ads} is the adsorptive equilibrium constant; T stands for the thermodynamic temperature; R is the universal gas constant and 55.5 represents the molar concentration of water in solution. Figure 7 shows the plot of C/θ against inhibitor concentration C at 303 K and the expected linear relationship is obtained for compounds with excellent correlation coefficients (R^2), confirming the validity of this approach.

The slopes of the straight lines are even, signifying that adsorbed inhibitor molecules form monolayer on the mild steel surface and there is no interface among the adsorbed inhibitor molecules. From the DG values less than -20 kJ/mol means

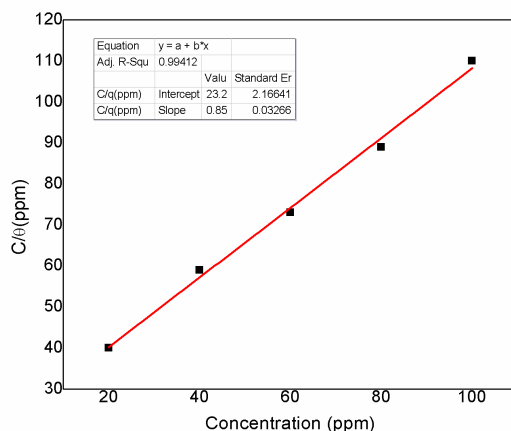


Fig 7. Adsorption isotherm of NMPP on mild steel

physical adsorption (intermolecular forces between adsorbent and adsorbate) and values more than -40 kJ/mol specifies that a chemisorption process (the formation of coordination bonds between the inhibitor molecules and iron atoms of steel surface). The calculated ΔG^0_{ads} values such as -33.3, -35.5, -37.3 and -39.0 obtained in the temperatures 303, 313, 323 and 333 K respectively. Hence, this adsorption isotherm model exhibits the chemisorptions phenomenon.

The Gibbs-Helmholtz equation measures the enthalpy of adsorption (ΔH^0_{ads}) as follows,

$$\left(\frac{\Delta G/T}{\Delta T}\right)P = \frac{H}{T^2} \left(\frac{\Delta G/T}{\Delta T}\right)P = \frac{H}{T^2} \tag{3.5}$$

The reordered form of the above equation is as follows. Figure 8 describes a plot of $\Delta G^0_{ads}/T$ against $1000/T$ with a slope value equal to ΔH^0_{ads} (Table 5). Generally, the values of ΔH^0_{ads} reach -100 kJ/mol include the process of chemisorption⁽²⁶⁾. In this work, we find that the magnitude of adsorption enthalpy is -102 kJ/mol and its indicates that the inhibitor has been chemically adsorbed on mild steel surfaces.

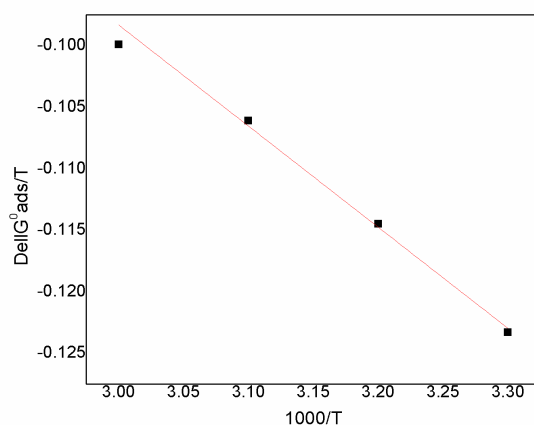


Fig 8. Enthalpy of adsorption (a plot of $\Delta G^0_{ads}/T$ against $1000/T$) (80 ppm NMPP inhibitor concentration)

Table 5. Plot of $\Delta G^{\circ}_{ads}/T$ against $1000/T$ with 80 ppm of NPPMPQC

S.No	Temperature	ΔG°_{ads} (KJ mol ⁻¹)	$\Delta G^{\circ}_{ads}/T$	ΔH°_{ads} (KJ mol ⁻¹)
1	303	-33.3	-0.0999	-102
2	313	-35.5	-0.1061	
3	323	-37.1	-0.1145	
4	333	-39.0	-0.1233	

3.3.5 Surface properties analysis

The surface morphology of the NMPP inhibitor and mild steel surface interacted materials were carried out using HR-SEM analysis (Figure 9). The HR-SEM images exposed those individual surfaces aggregates particle were composed by a collection of elongated particles of various size and shapes shown in Figure 9 a and b.

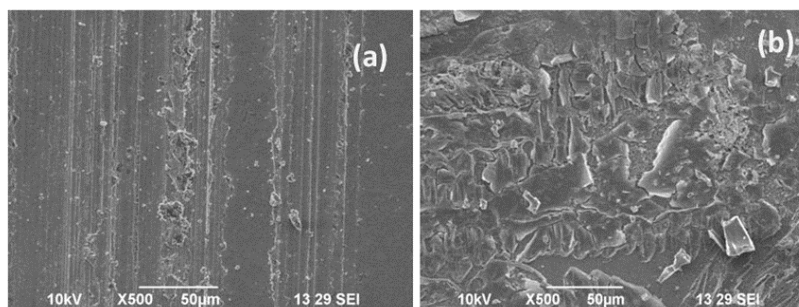


Fig 9. HR-SEM micrographs of (a) bare mild steel, (b) mild steel (MS) interacted NMPP surfaces

Figure 9 depicts the characteristics of the mild steel (MS) surface areas under different circumstances. The characteristic picture of MS surfaces after scratching is shown in Figure 9(a). Figure 9(b) depict the mild steel surfaces immersed in 1 N HCl with 80 ppm of NMPP adhered mild steel surface in 1 N HCl.

The results of the HR-SEM images exposed those individual surfaces aggregates particle were composed by a collection of elongated particles of various size and shapes. There are no apparent corrosion holes found and portions of the cleaned-out trench is still discernible. As a result, they show that the addition of NMPP to a solution of 1N HCl acid can effectively suppress the corrosion of mild steel by correlating the SEM images.

4 Conclusion

The corrosion rates and inhibition efficiencies of mild steel were monitored and controlled in 1.0 N HCl solutions at different temperatures without and with various concentrations of new synthesized piprazene (NMPP) derivatives. The NMPP inhibitor chemical structure could be confirmed by using FTIR analysis. Chemical (weight loss) methods were employed for the measuring the corrosion inhibition. The corrosion inhibition efficiency increased with the increase in inhibitor concentrations, with the corrosion inhibition efficiency reaching 88.34% at a concentration of 80 ppm at room temperature. SEM results showed that the corrosion inhibitor adsorbed on the surface of mild steel and formed a dense protective film. From the corrosion inhibition results, NMPP-metal interaction may be following the Langmuir adsorption isotherm. In perspective, the rest to be done is to improve the inhibitory power of NMPP by synergism with another compound. In conclusion, organic corrosion inhibitors play a crucial role in preventing metal corrosion. Further research is needed to better understand the mechanisms of organic inhibitors and to improve their efficiency. The development of new and improved organic inhibitors will help to reduce the impact of corrosion on metal surfaces and increase the lifespan of metal structures.

5 Acknowledgements

The authors gratefully acknowledge the support received for this research work from the Department of Chemistry, Rajah Serfoji Government College, Affiliated to Bharathidasan University, Thanjur, Tamil Nadu, INDIA.

References

- Ahmed ESJ, Ganesh GM. A Comprehensive Overview on Corrosion in RCC and Its Prevention Using Various Green Corrosion Inhibitors. *Buildings*. 2022;12(10):1–48. Available from: <https://doi.org/10.3390/buildings12101682>.
- Tamalmani K, Husin H. Review on Corrosion Inhibitors for Oil and Gas Corrosion Issues. *Applied Sciences*. 2020;10(10):1–16. Available from: <https://doi.org/10.3390/app10103389>.
- Zakeri A, Bahmani E, Aghdam ASR. Plant extracts as sustainable and green corrosion inhibitors for protection of ferrous metals in corrosive media: A mini review. *Corrosion Communications*. 2022;5:25–38. Available from: <https://doi.org/10.1016/j.corcom.2022.03.002>.
- Chauhan DS, Quraishi MA, Sorour AA, Verma C. A review on corrosion inhibitors for high-pressure supercritical CO₂ environment: Challenges and opportunities. *Journal of Petroleum Science and Engineering*. 2022;215(Part B):110695. Available from: <https://doi.org/10.1016/j.petrol.2022.110695>.
- Olajire AA. Recent advances on the treatment technology of oil and gas produced water for sustainable energy industry-mechanistic aspects and process chemistry perspectives. *Chemical Engineering Journal Advances*. 2020;4:100049. Available from: <https://doi.org/10.1016/j.cej.2020.100049>.
- Al-Amiery AA, Al-Azzawi WK, Isahak WNRW. Isatin Schiff base is an effective corrosion inhibitor for mild steel in hydrochloric acid solution: gravimetric, electrochemical, and computational investigation. *Scientific Reports*. 2022;12(1):1–18. Available from: <https://doi.org/10.1038/s41598-022-22611-4>.
- Talat R, Asghar MA, Tariq I, Akhter Z, Liaqat F, Nadeem L, et al. Evaluating the Corrosion Inhibition Efficiency of Pyridinium-Based Cationic Surfactants for EN3B Mild Steel in Acidic-Chloride Media. *Coatings*. 2022;12(11):1–25. Available from: <https://doi.org/10.3390/coatings12111701>.
- Gurjar S, Sharma SK, Sharma AK, Ratnani S. Performance of imidazolium based ionic liquids as corrosion inhibitors in acidic medium: A review. *Applied Surface Science Advances*. 2021;6:1–25. Available from: <https://doi.org/10.1016/j.apsadv.2021.100170>.
- Chaouiki A, Chafiq M, Ko YG, Al-Moubaraki AH, Thari FZ, Salghi R, et al. Adsorption Mechanism of Eco-Friendly Corrosion Inhibitors for Exceptional Corrosion Protection of Carbon Steel: Electrochemical and First-Principles DFT Evaluations. *Metals*. 2022;12(10):1–19. Available from: <https://doi.org/10.3390/met12101598>.
- Hanoon MM, Resen AM, Al-Amiery AA, Kadhum A, Takriff MS. Theoretical and experimental studies on the corrosion inhibition potentials of 2-((6-methyl-2-ketoquinolin-3-yl)methylene)hydrazinecarbothioamide for mild steel in 1 M HCl. *Progress in Color, Colorants and Coatings*. 2022;15(1):11–23. Available from: https://pccc.icrc.ac.ir/article_81740.html.
- Shamsa A, Barmatov E, Hughes TL, Hua Y, Neville A, Barker R. Hydrolysis of imidazoline based corrosion inhibitor and effects on inhibition performance of X65 steel in CO₂ saturated brine. *Journal of Petroleum Science and Engineering*. 2022;208(Part B):1–12. Available from: <https://doi.org/10.1016/j.petrol.2021.109235>.
- Tazouti A, Errahmany N, Rbaa M, Galai M, Roufi Z, Tourir R, et al. Effect of hydrocarbon chain length for acid corrosion inhibition of mild steel by three 8-(n-bromo-R-alkoxy)quinoline derivatives: Experimental and theoretical investigations. *Journal of Molecular Structure*. 2021;1244:130976. Available from: <https://doi.org/10.1016/j.molstruc.2021.130976>.
- Singh A, Ansari KR, Banerjee P, Murmu M, Quraishi MA, Lin Y. Corrosion inhibition behavior of piperidinium based ionic liquids on Q235 steel in hydrochloric acid solution: Experimental, density functional theory and molecular dynamics study. *Colloids and Surfaces A: Physicochemical and Engineering Aspects*. 2021;623:126708. Available from: <https://doi.org/10.1016/j.colsurfa.2021.126708>.
- Palumbo G, Kollbek K, Wirecka R, Bernasik A, Górny M. Effect of CO₂ Partial Pressure on the Corrosion Inhibition of N80 Carbon Steel by Gum Arabic in a CO₂-Water Saline Environment for Shale Oil and Gas Industry. *Materials*. 2020;13(19):1–24. Available from: <https://doi.org/10.3390/ma13194245>.
- Praveen BM, Prasanna BM, Mallikarjuna NM, Jagadeesh MR, Hebbar N, Rashmi D. Investigation of anticorrosive behaviour of novel tert-butyl 4-[(4-methyl phenyl) carbonyl] piperazine-1-carboxylate for carbon steel in 1M HCl. *Heliyon*. 2021;7(2):1–9. Available from: <https://doi.org/10.1016/j.heliyon.2021.e06090>.
- Rezaeivala M, Karimi S, Sayin K, Tüzün B. Experimental and theoretical investigation of corrosion inhibition effect of two piperazine-based ligands on carbon steel in acidic media. *Colloids and Surfaces A: Physicochemical and Engineering Aspects*. 2022;641:128538. Available from: <https://doi.org/10.1016/j.colsurfa.2022.128538>.
- Anbalagan S, Ravishankar M, Sivakumar S, Sivakumar M, Krishna E. Synthesis, Characterization and Corrosion Inhibition study of N-(4-((4-(pyridin-2-yl) piperazin-1-yl) methyl) phenyl) quinoline-6-carboxamide on Mild Steel under HCl Solution. *Indian Journal Of Science And Technology*. 2023;16(11):803–815. Available from: <https://doi.org/10.17485/IJST/v16i11.2364>.
- Ranjith PK, Ignatious A, Panicker CY, Sureshkumar B, Armakovic S, Armakovic SJ, et al. Spectroscopic investigations, DFT calculations, molecular docking and MD simulations of 3-[(4-Carboxyphenyl) carbamoyl]-4-hydroxy-2-oxo-1, 2-dihydroxy quinoline-6-carboxylic acid. *Journal of Molecular Structure*. 2022;1264:133315. Available from: <https://doi.org/10.1016/j.molstruc.2022.133315>.
- Chen Y, Chen Z, Zhuo Y. Newly Synthesized Morpholinyl Mannich Bases as Corrosion Inhibitors for N80 Steel in Acid. *Materials*. 2022;15(12):1–15. Available from: <https://doi.org/10.3390/ma15124218>.
- Gupta SK, Mitra RK, Yadav M, Dagdag O, Berisha A, Mamba BB, et al. Electrochemical, surface morphological and computational evaluation on carbonylhydrazide Schiff bases as corrosion inhibitor for mild steel in acidic medium. *Scientific Reports*. 2023;13(1):1–21. Available from: <https://doi.org/10.1038/s41598-023-41975-9>.
- Kateel LD, Frank PV, Alva VDP, Vd A. Corrosion Inhibition of Mild Steel in Hydrochloric Acid Medium Using Schiff Base Synthesized by Green Approach. *Surface Engineering Applied Electrochemistry*. 2023;59(4):511–522. Available from: <https://www.springerprofessional.de/en/corrosion-inhibition-of-mild-steel-in-hydrochloric-acid-medium-u/26006602>.
- Oubaaqa M, Ouakki M, Rbaa M, Benhiba F, Galai M, Idouhli R, et al. Experimental and theoretical investigation of corrosion inhibition effect of two 8-hydroxyquinoline carbonitrile derivatives on mild steel in 1 M HCl solution. *Journal of Physics and Chemistry of Solids*. 2022;169:110866. Available from: <https://doi.org/10.1016/j.jpics.2022.110866>.
- Aziz IAA, Annon IA, Abdulkareem MH, Hanoon MM, Alkaabi MH, Shaker LM, et al. Insights into Corrosion Inhibition Behavior of a 5-Mercapto-1, 2, 4-triazole Derivative for Mild Steel in Hydrochloric Acid Solution: Experimental and DFT Studies. *Lubricants*. 2021;9(12):1–14. Available from: <https://doi.org/10.3390/lubricants9120122>.
- Chen Y, Chen Z, Zhuo Y. Newly Synthesized Morpholinyl Mannich Bases as Corrosion Inhibitors for N80 Steel in Acid Environment. *Materials*. 2022;15(12):1–15. Available from: <https://doi.org/10.3390/ma15124218>.
- Guruprasad AM, Sachin HP, Swetha GA, Prasanna BM. Corrosion inhibition of zinc in 0.1 M hydrochloric acid medium with clotrimazole: Experimental, theoretical and quantum studies. *Surfaces and Interfaces*. 2020;19:100478. Available from: <https://doi.org/10.1016/j.surfin.2020.100478>.

- 26) Praveen BM, Alhadhrami ABM, Prasanna BM, Hebbar N, Prabhu R. Anti-Corrosion Behavior of Olmesartan for Soft-Cast Steel in 1 mol dm⁻³ HCl. *Coatings*. 2021;11(8):1-18. Available from: <https://doi.org/10.3390/coatings11080965>.